TISSUE ENGINEERING: Part C
Volume 21, Number 9, 2015

DOI: 10.1089/ten.tec.2014.0643

termis
Tissue Engineering
& Regenerative Medicine
International Society

METHODS ARTICLE

Dual Delivery of EPO and BMP2 from a Novel Modular Poly-ε-Caprolactone Construct to Increase the Bone Formation in Prefabricated Bone Flaps

Janki Jayesh Patel, MS,[1] Jane E. Modes,[1] Colleen L. Flanagan, MSE,[1]
Paul H. Krebsbach, DDS, PhD,[2] Sean P. Edwards, DDS, MD,[3] and Scott J. Hollister, PhD[1]

Poly-ε-caprolactone (PCL) is a biocompatible polymer that has mechanical properties suitable for bone tissue engineering; however, it must be integrated with biologics to stimulate bone formation. Bone morphogenetic protein-2 (BMP2) delivered from PCL produces bone when implanted subcutaneously, and erythropoietin (EPO) works synergistically with BMP2. In this study, EPO and BMP2 are adsorbed separately on two 3D-printed PCL scaffold modules that are assembled for codelivery on a single scaffold structure. This assembled modular PCL scaffold with dual BMP2 and EPO delivery was shown to increase bone growth in an ectopic location when compared with BMP2 delivery along a replicate scaffold structure. EPO (200 IU/mL) and BMP2 (65 μg/mL) were adsorbed onto the outer and inner portions of a modular scaffold, respectively. Protein binding and release studies were first quantified. Subsequently, EPO + BMP2 and BMP2 scaffolds were implanted subcutaneously in mice for 4 and 8 weeks, and the regenerated bone was analyzed with microcomputed tomography and histology; 8.6 ± 1.4 μg BMP2 (22%) and 140 ± 29 IU EPO (69.8%) bound to the scaffold and < 1% BMP2 and 83% EPO was released in 7 days. Increased endothelial cell proliferation on EPO-adsorbed PCL discs indicated protein bioactivity. At 4 and 8 weeks, dual BMP2 and EPO delivery regenerated more bone (5.1 ± 1.1 and $5.5 \pm 1.6\,mm^3$) than BMP2 alone (3.8 ± 1.1 and $4.3 \pm 1.7\,mm^3$). BMP2 and EPO scaffolds had more ingrowth ($1.4\% \pm 0.6\%$) in the outer module when compared with BMP2 ($0.8\% \pm 0.3\%$) at 4 weeks. Dual delivery produced more dense cellular marrow, while BMP2 had more fatty marrow. Dual EPO and BMP2 delivery is a potential method to regenerate bone faster for prefabricated flaps.

Introduction

The gold standard for treating a large craniofacial bone defect is an autograft usually taken from the fibula or iliac crest. This defect can be caused by trauma, tumor resection, or developmental abnormalities. Methods to tissue engineer a bone flap are under investigation to overcome the drawbacks associated with autografts, including high donor site morbidity, increased risk of infection, and defect geometry mismatch. Tissue engineering a flap can be conducted *in vitro* or *in vivo*. *In vitro*, the scaffold with added cells would be placed in an external bioreactor. However, regenerating a large bone volume (BV) *in vitro* is time-consuming, and it is difficult to maintain optimal nutrient perfusion throughout the scaffold.[1] As an alternative, we propose the process of prefabricating a bone flap *in vivo* by implanting a patient-specific 3D-printed scaffold with associated biologics into the back muscle, and then transplanting it to the defect site after a maturation period as a boney vascularized flap. Previous studies have created prefabricated flaps by utilizing a titanium cage, filling it with Bio-Oss blocks soaked in bone morphogenetic protein-7 (BMP7), adding cells, and implanting the construct inside of the patient's latissimus dorsi muscle.[2–10] After 6 weeks, the implant was transferred to the defect site, but due to loading issues, the implant fractured and failed.[2]

We are looking to advance this prefabrication process by integrating patient-specific design, 3D printing, and multiple biologics delivery.[11] Poly-ε-caprolactone (PCL) is a biocompatible and biodegradable polymer, which can be 3D printed using a selective laser sintering (SLS) manufacturing technique to produce scaffolds of complex geometry based on the patient's computed tomography (CT) scan.[12] SLS printing can reproducibly create scaffolds with designed porosity, mechanical properties, and permeability. Furthermore, PCL leads to less inflammation and generates less

[1]Department of Biomedical Engineering, [2]School of Dentistry, and [3]Department of Oral and Maxillofacial Surgery, University of Michigan, Ann Arbor, Michigan.

acidic by-products when compared with polylactic acid-based copolymers.[13] PCL is also currently utilized in 510(k) approved cranioplasty bone filling applications.[14,15] Previously, in our laboratory, we found that BMP2 adsorbed onto a porous PCL scaffold in a clinically applicable setting (1 h protein exposure at room temperature) regenerates bone when implanted subcutaneously in a murine model.[16]

A flap needed for a large defect would need a large BV as well as a rich vascular network to supply nutrients to the growing bone, remove waste, and form a vascular pedicle that can be connected to a vessel at the defect site. Furthermore, for oncology patients awaiting adjuvant therapy, the speed at which bone is regenerated in the donor muscle site is essential. We hope to increase the regenerated BV at an earlier time point when compared with BMP2 delivery alone by delivering erythropoietin (EPO) along with the BMP2 in a clinically applicable manner.

EPO is a protein that stimulates erythropoiesis, acts as a cytokine for red blood cell precursors in the bone marrow, and has been shown to promote angiogenesis in a variety of tissues.[17] EPO indirectly impacts bone healing by influencing hematopoietic stem cells to produce BMP2.[18–20] *In vitro*, EPO has been shown to directly influence mesenchymal stem cells to differentiate into osteoblasts, indicating that they must have EPO receptors.[19,20] EPO receptors are also expressed on endothelial cells, neurons, and trophoblast cells.[19] EPO has been used clinically to treat anemia and has some angiogenic properties.[21–23]

EPO can be delivered systemically; however, drawbacks include serious side effects, such as increased blood viscosity, hypertension, and thromboembolic events.[21,24,25] To avoid the drawbacks associated with systemic delivery, some studies have looked at local EPO delivery. Kobayashi *et al.* delivered EPO using a gelatin hydrogel at the surface of a rabbit heart,[26] and Chen *et al.* delivered EPO using fibrin gel to increase neovascularization.[27] Interactions between EPO and BMP2 have been studied *in vitro*[19,20] and *in vivo*,[28,29] and results have shown synergistic effects on bone formation.

Although these dual delivery results are promising, there is limited knowledge on the effects of locally delivering both BMP2 and EPO on ectopic bone regeneration for prefabricated flap applications. In addition, the use of 3D-printed modular delivery of multiple growth factors has not been reported. In this study, we investigated the *in vitro* binding, release, and bioactivity of adsorbed BMP2 and EPO from a modular PCL scaffold and, furthermore, analyzed the regenerated ectopic BV and spatial distribution.

Materials and Method

PCL scaffold fabrication

Solid PCL discs (6 mm diameter, 2 mm height) and 44% porous inner (3.5 mm sides, 4.3 mm height, 106 mm^2 surface area [SA]) and 79% porous outer (7 mm sides, 4.3 mm height, 357 mm^2 SA) PCL scaffolds were fabricated through SLS using a Formiga P100 (EOS, Inc.) (Fig. 1). Previously, in this laboratory, we used 70% porous scaffolds that had a different geometry.[16] Due to limitations, including laser spot size and a new scaffold geometry requiring the two porous modules to fit together tightly, two pore sizes were needed. PCL powder (43–50 kDa; Polysciences) was mixed with 4 wt% hydroxyapatite (Plasma Biotal Limited). After manufacturing, the scaffolds were air blasted, sonicated in 70% ethanol (EtOH), sterilized in 0.22 μm filtered 70% EtOH, and air-dried under sterile conditions.

EPO binding to PCL scaffolds

One hundred micrograms of EPO (Creative Biomart) was reconstituted in 1 mL sterile Dulbecco's phosphate-buffered saline (DPBS) to result in 12,000 IU/mL (0.1 mg/mL). The stock solution was further diluted to the desired concentrations in DPBS. The outer modular scaffolds were placed in an ultra-low bind 24-well plate (Costar) and washed in DPBS to wet the surface. Scaffolds were then exposed to 1 mL EPO solution at room temperature for 1 h ($n=3$); 100 IU/mL per PCL disc was used for bioactivity studies to conserve materials, and 200 IU/mL per scaffold was used for binding, release, and *in vivo* studies. Finally, scaffold modules were washed in DPBS to remove loosely bound protein. The washes and the remaining EPO solution following the exposure were collected to indirectly quantify the EPO remaining in the solution utilizing a protein quantification kit (Fluoroprofile; Sigma). A standard curve was created from 2.5 to 0 μg/mL (300–0 IU/mL). A volume of

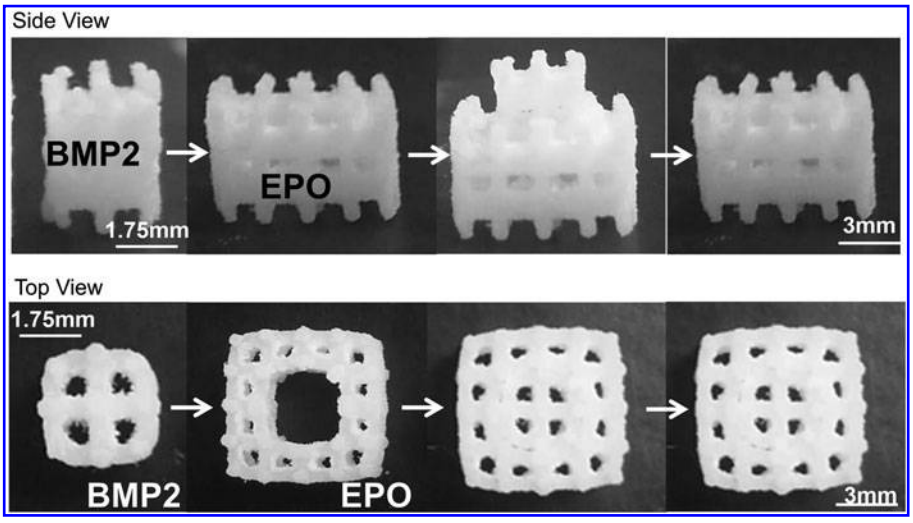

FIG. 1. Modular scaffold assembly. BMP2 was adsorbed onto the inner scaffold module and EPO was adsorbed onto the outer scaffold module. The two scaffolds were then assembled. BMP2, bone morphogenetic protein-2; EPO, erythropoietin.

working solution (Fluoroprofile reagent and buffer) was added to an equal volume of unknown EPO sample. Samples were read in triplicates with a fluorometric reader (520 nm excitation, 620 emission).

$$EPO\ Bound\ (IU) = (EPO\ exposed\ to\ scaffold) - (EPO\ in\ remaining\ solution + EPO\ in\ washes)$$

BMP2 binding and quantification

BMP2 was adsorbed onto the inner scaffold modules as previously described.[16] Briefly, 1 mg lyophilized BMP2 (BMP2-01H; Creative Biomart) was dissolved in 1 mL of 20 mM acetic acid and it was then further diluted in BuPH (No. 28372; Pierce) buffer with 0.1 M EDTA (pH 7.0) to 65 μg/mL. A BMP2 ELISA (Peprotech), specific for *Escherichia Coli*-derived BMP2, was used to quantify the protein content in the 65 μg/mL BMP2 solution (average detected concentration was 28.12 ± 4.6 μg/mL) and the binding studies were normalized to this value. Briefly, the inner scaffold modules were washed in BuPH buffer (pH 7.2), followed by BuPH + 0.1 M EDTA buffer to wet the surface, exposed to 1 mL of 65 μg/mL BMP2 for 1 h at 23°C ($n = 3$), and washed in water (diH_2O) before use. The washes and the BMP2 solution remaining after exposure were collected, 1% bovine serum albumin (BSA) was added to result in 0.1% BSA content, and samples were stored at −80°C until ELISA analysis for BMP2 content.

$$BMP2\ Bound\ (\mu g) = (BMP2\ in\ original\ solution\ detected\ by\ ELISA) - (BMP2\ in\ remaining\ solution + BMP2\ in\ washes)$$

The ELISA was carried out according to the manufacturer's directions.

Release kinetics

The outer scaffold modules with adsorbed EPO were manually assembled with the inner scaffold modules that had no BMP2 adsorbed (Fig. 1). Constructs were submerged in 1 mL DPBS and incubated at 37°C, 95% humidity, 5% CO_2. The supernatant was collected and replenished at 1, 2, 3, 5, and 7 days after initial exposure. Samples were stored at −80°C until Fluoroprofile assay analysis for protein content.

The inner scaffold modules with adsorbed BMP2 were assembled with an outer module that had no adsorbed EPO, submerged in 1 mL DPBS, and incubated at 37°C, 95% humidity, 5% CO_2. The supernatant was collected and replenished 1, 2, 3, 5, and 7 days after initial exposure. Supernatants with a final 0.1% BSA content were stored at −80°C until BMP2 quantification with an ELISA.

Adsorbed EPO bioactivity

Previous studies in the laboratory show that BMP2 adsorbed to the PCL surface maintains bioactivity as seen by C2C12 cell alkaline phosphatase production.[16] In this study, endothelial cell proliferation was used to indicate EPO bioactivity as done in other studies.[30–32] A disc geometry with a flat surface was used for this assay due to a well-defined surface area and a simple geometry. This assay's goal was to assess the protein's bioactivity and not the extent of bioactivity. Second passage human umbilical vein endothelial cells (HUVECs) were cultured in EGM-2 growth medium (CC-3162; Lonza) for 4 days at 37°C, 95% humidity, 5% CO_2. Cells were trypsinized using 0.05% Trypsin with EDTA (Gibco) and quantified with an automatic cell counter—MoxieZ (Orflo).

EGM-2 growth media (1 mL) were added to PCL discs exposed to 100 IU EPO ($n = 4$), and 2.0×10^4 HUVECs were seeded on each disc (11,765 cells/cm^2). Cells seeded onto discs without EPO exposure and PCL discs without cells served as the negative control. After 72 h of static culture, the cell medium was replaced with 500 μL of fresh EGM-2 medium and 100 μL of MTS solution (CellTiter96 Aqueous One Solution; Promega) was added per well. Constructs were incubated with the MTS reagent at 37°C for 4 h and triplicates for each condition were read at 490 nm on a microplate reader.

Cells were also seeded at 0, 2×10^4, 4×10^4, 8×10^4, and 16×10^4 cells per well in triplicate to create a standard curve (cell number vs. absorbance reading). After 1 h, 100 μL of MTS solution was added to the 500 μL EGM medium in each well, and the absorbance was read at 490 nm on a microplate reader.

In vivo *bioactivity: subcutaneous implantation*

BMP2 inner scaffold modules (adsorbed with 65 μg/mL BMP2) were assembled with outer scaffold modules (adsorbed with 200 IU/mL EPO) for the dual delivery BMP2 + EPO group. The negative control was outer modules with 200 IU/mL EPO adsorbed and no BMP2 adsorbed onto the inner modules (EPO group). The positive control was inner modules with 65 μg/mL BMP2 adsorbed and no EPO adsorbed onto the outer modules (BMP2 group). Scaffolds from each group were implanted subcutaneously in 5- to 6-week-old female C57BL/6N mice.

The dorsal hair was shaved and an incision was made in the back. Two subcutaneous pockets were created, one on each side, and a scaffold was placed into each pocket. Scaffolds were randomly assigned a side to be implanted such that half of the samples from each group were implanted on both the right and left sides. The positive control (the BMP2 group) was implanted in a parallel study such that BMP2 + EPO and BMP2 scaffolds were not implanted in the same mouse. Mice were sacrificed at 4 and 8 weeks postsurgery to assess bone regeneration. The explanted specimens were placed in Z-Fix (Anatech) overnight, washed in diH_2O for 24 h, and stored in 70% EtOH until assays were performed. Table 1 describes the total sample numbers and the number of samples used for each specific analysis method. This study was conducted in compliance with the regulations set forth by the University Committee on Use and Care of Animals at the University of Michigan.

Microcomputed tomography

Fixed scaffolds were scanned in water with a high-resolution (16 μm) micro-CT (microCT) scanner (Scanco Medical), and the scans were calibrated to Hounsfield units (HU). BV was defined at a 1050 HU threshold using Microview software (Parallax Innovations). Tissue mineral

Table 1. Sample Numbers for *In Vivo* Analysis. Number of Samples Used in Explanted Specimen Analysis Methods

	μCT scan		*Histology*		*Total samples*	
Group	*4 week*	*8 week*	*4 week*	*8 week*	*4 week*	*8 week*
BMP2 + EPO	9	8	3	2	9	8
BMP2	8	9	2	2	8	9
EPO	9	8	3	2	9	8

density (TMD) was determined using exported grayscale data. The total scaffold region was represented as a cubical region of interest (ROI) defined as $7 \times 7 \times 4.3$ mm height. An ROI defining the inner scaffold module ($3.5 \times 3 \times 4.3$ mm height) was used to determine bone formation within the module. Bone regenerated in the outside scaffold module was calculated as the inner scaffold module BV subtracted from the total scaffold BV. The total, inner module, and outer module scaffold bone ingrowth was calculated as the BV divided by the available pore volume in each region. Available pore volume was calculated from the porosity of each module based on the microCT image of an assembled modular scaffold (preimplantation) scanned in air. To determine the amount of bone formed in the central region of the inner module pores instead of on the PCL surface, a 0.6750-mm-diameter, 4.3-mm-height cylinder ROI was created in all four vertical pores, and the total BV in inner module pores was calculated. TMD was calculated for the total, inner module, and outer module scaffolds.

Histology

Fixed scaffolds from each group were decalcified with RDO (Apex Engineering Products Corporation), processed, and embedded in paraffin. Samples were then sectioned at 7 μm thickness using a MICRON HM 325 (Thermo Scientific) and slides were incubated at 37°C overnight to dry. Sections were stained with hematoxylin and eosin (H&E) to visualize cells, tissue matrix, blood vessels, and general tissue morphology. Sections were imaged with a 4× objective.

Statistical analysis

Data are expressed as mean ± standard deviation of the mean. An analysis of variance was used to determine statistical significance between groups. A p-value less than 0.05 ($\alpha < 0.05$) was considered statistically significant on a 95% confidence interval.

Results

Protein binding and release kinetics

After 1 h of protein exposure, 139.6 ± 28.6 IU EPO (69.8%) and 8.56 ± 1.4 μg BMP2 (22%) bound to the outer and inner scaffold modules, respectively. After 7 days, 0.0311 ± 0.0053 μg BMP2 (<1%) and 119.2 ± 29.4 IU EPO were released (85%) from the PCL surface (Fig. 2A, C). For both proteins, there was a relatively small burst release in the first 2 days of 45.8 ± 24 IU EPO (32.8%) and 0.017 ± 0.007 μg BMP2 (0.2%) (Fig. 2B, D). HUVECs seeded on EPO-adsorbed PCL discs experienced increased cell proliferation ($2.4 \pm 0.3 \times 10^4$ cells/disc) when compared with

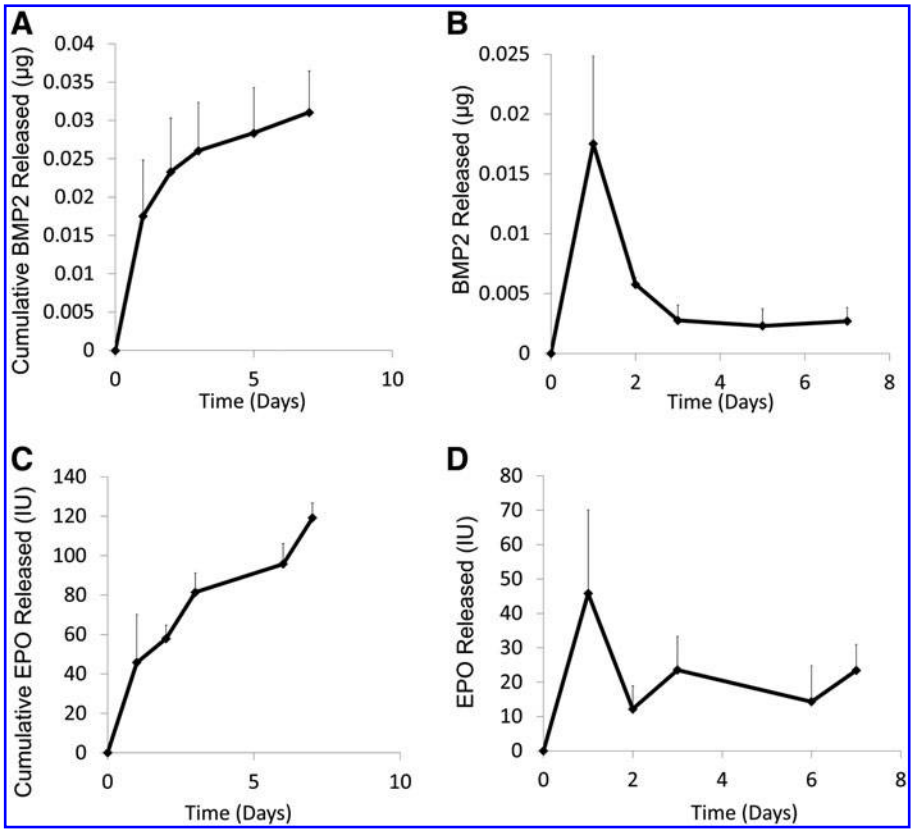

FIG. 2. Protein release profiles. **(A)** BMP2 cumulative release profile. After 7 days, 0.0311 ± 0.0053 μg BMP2 was released into phosphate-buffered saline at 37°C. **(B)** BMP2 release. A small burst release occurred in the first 2 days, followed by sustained release. **(C)** EPO cumulative release profile. After 7 days, 119.2 ± 29.4 IU of the 139.6 ± 28.6 IU that was bound was released. **(D)** EPO released over 7 days with a small burst release in the first 2 days. ($n = 3$/group).

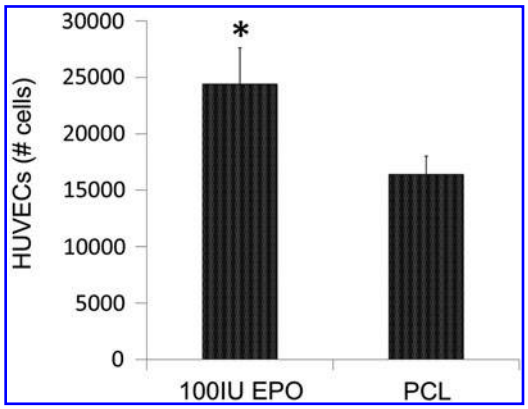

FIG. 3. Adsorbed EPO bioactivity. HUVECs seeded on the PCL disc exposed to EPO showed increased levels of proliferation. $n=4$; $^*p<0.05$. HUVEC, human umbilical vein endothelial cells; PCL, poly-ε-caprolactone.

cells seeded on PCL discs without any protein exposure ($1.6\pm0.1\times10^4$ cells/disc) (Fig. 3).

Microcomputed tomography: bone volume

Visual analysis of the microCT scans shows that BMP2 only groups regenerated bone (indicated by the red arrow) localized mainly on the inner module, which had been adsorbed with the osteogenic factor (Fig. 4A). The darker areas are the pore space indicated by the red circle, and the light gray areas are the PCL scaffold (red star). The BMP2+EPO group regenerated bone not only in the inner module but also in the surrounding outer module. At both time points, the dual delivery BMP2+EPO group produced more bone than the BMP2 group. The EPO group regenerated little to no visible bone. Microview software was utilized to quantify the BV observed in the microCT scans. At 4 weeks, the dual delivery group regenerated significantly more total bone ($5.1\pm1.1\,mm^3$) than the BMP2 group ($3.8\pm1.1\,mm^3$) ($p=0.019$) (Fig. 4B). BMP2+EPO had more bone regenerated in the inner module, although it was not significantly more ($p=0.068$), and in the outer module ($p=0.276$). At 8 weeks, a similar trend was observed; however, there was no significant difference between dual and single growth factor delivery ($p=0.279$). Overall, BMP2+EPO regenerated more total, inner module, and outer module BV than the BMP2 group. At both time points, the BMP2 and BMP2+EPO groups had significantly more BV than the EPO group (less than $0.2\,mm^3$).

Bone ingrowth and TMD analysis

Bone ingrowth analysis was not conducted for the EPO group because little to no BV was detected. At 4 and 8 weeks, both of the BMP2+EPO and BMP2 groups had the same BV form in the inner module pores (Fig. 5A). At 4 weeks, BMP2+EPO had significantly more bone ingrowth in the outer module ($1.44\%\pm0.6\%$) when compared with the BMP2 group ($0.81\%\pm0.3\%$) ($p=0.018$) (Fig. 5B). The increased bone ingrowth for dual delivery also occurred at 4 weeks in the inner module; however, the increase was not significant ($p=0.067$). With respect to the total scaffold, BMP2+EPO had significantly more ingrowth than BMP2 at 4 weeks ($p=0.03$). There were no significant differences in ingrowth between the two groups throughout the scaffold at 8 weeks (Fig. 5B).

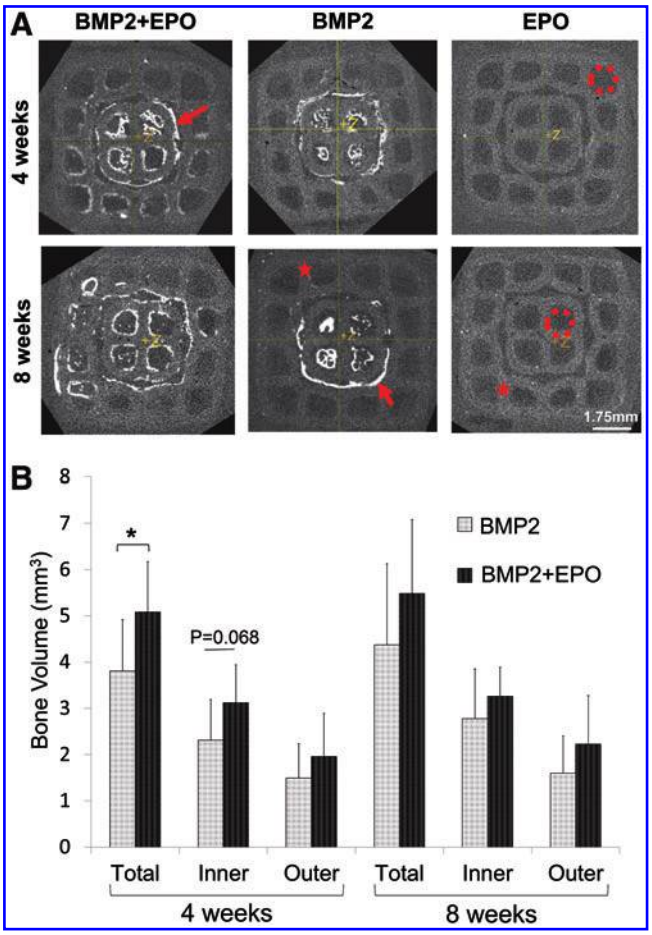

FIG. 4. MicroCT analysis of regenerated bone. **(A)** Representative microCT images. The BMP2 group regenerated bone localized to the inner module, and EPO+BMP2 regenerated bone in the outer module pores as well as in the inner module. *Red arrow*=bone, *red circle*=pore space, *red star*=PCL scaffold. **(B)** EPO+BMP2 resulted in significantly more total regenerated bone compared with the BMP2 group at 4 weeks ($^*p<0.05$). MicroCT, microcomputed tomography. Color images available online at www.liebertpub.com/tec

TMD analysis showed that regenerated bone in the BMP2 group was significantly more mineralized than that of the BMP2+EPO group at 4 weeks (505.8 ± 31.1 vs. 440.18 ± 29.1 mg HA/cm^3; $p=0.0001$) and at 8 weeks (583.0 ± 35.7 vs. 501.7 ± 40.6 mg HA/cm^3; $p=0.001$). Further analysis of inner and outer scaffold module TMD at 4 weeks showed that the BMP2 group had significantly more dense bone in the outer module when compared with the inner module. The BMP2+EPO group had no difference in TMD between the two scaffold modules. At 8 weeks, both BMP2 and BMP2+EPO groups had uniform TMD throughout the scaffold (Fig. 6).

Histology

Histology staining showed bone marrow, osteoid, blood vessels, and osteocytes embedded in bone matrix for the

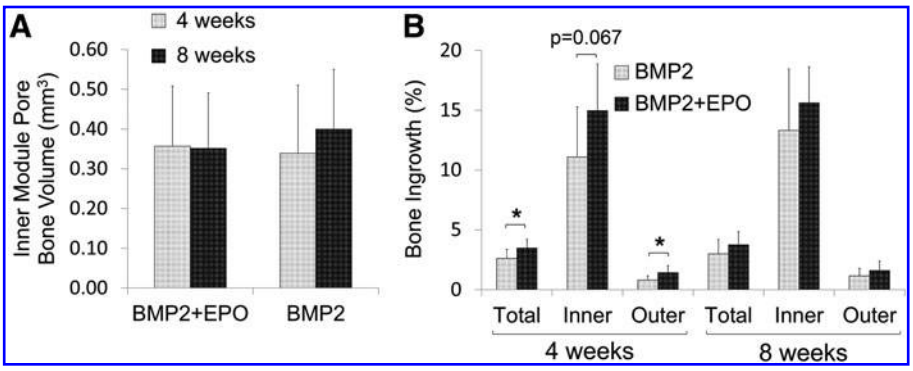

FIG. 5. Pore bone growth and scaffold ingrowth. **(A)** Bone volume formed inside of the inner module vertical pores was quantified at a 1050 HU threshold. Pore ROIs used were 4.3 mm in height, 0.670 mm in diameter. **(B)** Dual delivery had higher bone ingrowth in the total, inner module, and outer module at 4 weeks ($*p < 0.05$). HU, Hounsfield units; ROI, region of interest.

BMP2 + EPO and BMP2 groups (Fig. 7). The dual delivery group had more dense cellular marrow and the BMP2 group seemed to have more fatty marrow. The EPO group comprised mostly fibrous tissue. For both groups, osteocytes were embedded in the osteoid and osteoblasts were located at the periphery of forming bone.

Discussion

Medtronic's Infuse™ product has been FDA approved for BMP2 delivery from a collagen type 1 sponge for a variety of applications: spinal fusion, the treatment of open tibial fractures, sinus augmentation, and dental procedures.[33] Due to the BMP2 short half-life, a 1.5 mg/mL BMP2 dose was needed (greatly exceeding native concentrations of 18.8–22 pg/mL), which resulted in a large burst release during the first 2–3 days causing adverse reactions in some patients.[34] Amgen's product EPOGEN® is also FDA approved and uses the EPO protein to increase red blood cell levels caused by chronic kidney disease in anemic patients. This administration avoids the need for red blood cell transfusions.[35,36] Since these proteins are already FDA approved, the next step of dual delivery is feasible, although some regulatory hurdles would increase.

Although local BMP2 delivery from various scaffolds in a subcutaneous model has been widely studied for bone tissue engineering applications, there are very few investigations into local EPO delivery. EPO has been delivered through injectable hydrogels,[37,38] gelatin,[26] and fibrin gel[27] for angiogenesis studies; however, only one study of which we are aware has locally delivered EPO and BMP2 from a porogen-leached protein microbubble polyglycolic acid (PLGA) scaffold to assess bone regeneration in a calvarial defect model.[29] In another study, BMP2 was delivered from a collagen scaffold implanted in a rat calvarial defect, and EPO was injected subcutaneously at the defect site every other day for 2 weeks. After 6 weeks, the dual delivery group had a higher BV fraction than the BMP2 alone group.[28] There is limited to no knowledge of the binding and release of adsorbed EPO on PCL and, furthermore, the effect of dual EPO and BMP2 delivery on bone regenerated in an ectopic location for the application of prefabricated flaps is unknown.

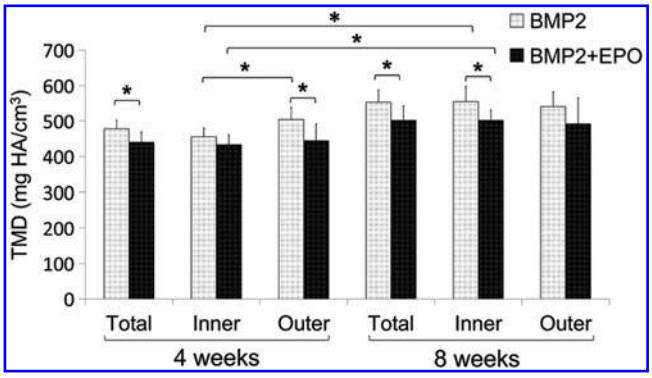

FIG. 6. TMD analysis of regenerated bone. TMD of the total, inner module, and outer module was determined using Microview software. At 4 weeks, the BMP2 group had more dense bone in the outer module and the dual delivery group had the same density bone throughout the scaffold ($*p < 0.05$). TMD, tissue mineral density.

In this study, we used adsorption as the protein-binding method to PCL due to the potential translational nature of this process. A short protein exposure time (<1 h) at room temperature before scaffold implantation is ideal for operating room environments. More complex processes that bind the protein outside of the operating room will face increased regulatory hurdles, such as sterilization, shelf life, and maintained efficacy studies. Additionally, in this study, a modular scaffold design is used, which is a novel method to deliver multiple growth factors. The two components are simple to assemble while maintaining their geometric complexity due to SLS manufacturing.

One hour adsorption resulted in 139.6 ± 28.6 IU EPO (69.8%) and 8.56 ± 1.4 μg BMP2 (22%) binding. After 7 days, less than 1% BMP2 was released. Even though this is a small amount, it is shown to be therapeutically relevant in the *in vivo* study. Since an ELISA was used to detect the protein, the remaining BMP2 could have released off the surface, but may have degraded, which would go undetected by the assay. Another explanation is that it may not have been released and required *in vivo* proteolytic activity to be released. As for EPO, 85% of the bound protein was released in the first week *in vitro*. Similarly, Fayed *et al.* incorporated EPO into PLGA nanoparticles, resulting in a 33% loading efficiency and 82% release over 24 h.[39] When delivered from chitosan nanoparticles, 30% was released in the first 48 h, and a total of 63% was released over 15 days in phosphate-buffered saline at 37°C.[40] EPO adsorbed onto dialysis bags resulted in less than 7% binding.[41] HUVECs proliferated significantly more on PCL discs with adsorbed EPO, indicating that the bound or released EPO was still bioactive. We have shown in previous studies that BMP2 released after adsorption onto PCL was still bioactive, as seen with alkaline phosphatase activity.[16] BMP2 was

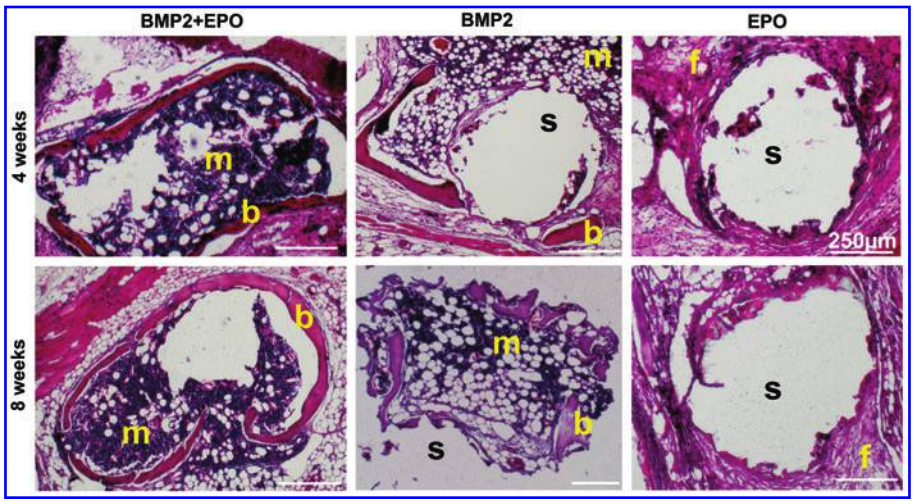

FIG. 7. Histology: H&E staining. BMP2+EPO and BMP2 groups showed osteoid, blood vessel, and marrow formation at both time points. The BMP2+EPO group had more dense cellular marrow and the BMP2 group had more fatty marrow. b, bone; m, marrow; s, scaffold; f, fibrous tissue; H&E, hematoxylin and eosin. Color images available online at www.liebertpub.com/tec

adsorbed onto the inner module because it is more challenging to regenerate bone at the scaffold's center. EPO is known to have angiogenic effects, and with its relatively faster release profile, developing vasculature in the outer module could deliver more cells to the BMP2 located at the center of the scaffold.

In vivo, a modular scaffold that delivered EPO combined with BMP2 produced significantly more total bone at 4 weeks when compared with the BMP2 group. This increased early bone formation is important for prefabricated flap applications because the flap would mature faster for oncology patients awaiting adjuvant therapy. At 8 weeks, the dual delivery group still had more bone than the BMP2 alone group; however, the increase was not significantly different. Upon visual inspection, the BMP2 group regenerated bone localized to the inner module area where the BMP2 was adsorbed. The BMP2+EPO group regenerated bone in both the outer and inner modules, indicating that the EPO influence was not spatially constricted to the outer module. It may have had a synergistic effect on bone production in adjacent areas. Since EPO was released rather quickly, it could have diffused to interact with migrating cells. Bone formation was also controlled and limited within the scaffold boundary. Dual delivery produced more bone than the BMP2 group, but the amount of bone that grew in the inner module pores was the same; therefore, dual delivery may have grown more bone on the surface of the pores.

Bone ingrowth analysis found that BMP2+EPO regenerated significantly more bone in the outer module available pore space at 4 weeks when compared with BMP2 alone. This increased bone growth seen with the dual delivery group could be explained by the synergistic effects between EPO and BMP2. EPO has shown to play a role in osteoclastogenesis and osteoclasts can recruit mesenchymal stem cells to the site of bone remodeling.[28] If EPO caused an initial increase in osteoclast numbers, this may have resulted in increased bone-forming cells recruited to the construct. Interestingly, although dual delivery had more bone than the BMP2 group, the BMP2 group had a higher TMD when compared with BMP2+EPO at both time points. One potential explanation for this difference could be that the dual delivery bone was forming faster than BMP2 alone and the osteoblasts may not have been mineralizing the osteoid at the same rate. Despite the difference, dual delivery resulted in uniform TMD throughout the scaffold in the range of native bone, whereas BMP2 had more dense bone in the outer module when compared with the inner module. With regard to developing a bone flap, having more bone with TMD in the normal range may be an advantage over less bone with higher mineral content overall. Gross tissue morphology analysis of explanted samples finds a more dense cellular marrow for the BMP2+EPO groups and a more fatty marrow for the BMP2 groups. This difference should be further investigated in future studies.

In this study, we successfully detected adsorbed EPO and BMP2 binding and release kinetics from a novel modular PCL scaffold. Once adsorbed to the surface, these proteins maintain bioactivity. These two proteins are already FDA approved for several clinical indications, and the simple binding process can be conducted in a clinically applicable environment (1 h of protein to scaffold exposure at room temperature). Furthermore, delivering EPO along with the osteogenic protein BMP2 resulted in increased bone regeneration in comparison with single BMP2 or EPO delivery. Since the implant is acellular when implanted, circulating mesenchymal stem cells and fibroblasts could be interacting with the delivered growth factors and inducing bone formation. Future studies should investigate the effects of altering the BMP2 and EPO dose ratios, and more studies could be completed to elucidate the mechanisms of EPO and BMP2 synergy to further optimize the dual delivery protocol.

Conclusions

The speed at which bone forms in a prefabricated flap is crucial for oncology patients awaiting adjuvant therapy. In this study, we have found that delivering EPO along with BMP2 could be a potential method to regenerate a greater BV at an earlier time point when compared with BMP2 alone delivery. Local dual delivery of EPO and BMP2 has not been investigated in depth, and delivering multiple biologics may advance the process of prefabricating flaps for skeletal reconstruction.

Acknowledgments

This research was funded by the Tissue Engineering at Michigan trainee T-32 grant, NIH R21 DE 022439, and NIH R01 AR 060892.

Disclosure Statement

Scott Hollister was a cofounder of Tissue Regeneration Systems (TRS), but is no longer affiliated with TRS.

References

1. Bhumiratana, S., and Vunjak-Novakovic, G. Concise review: personalized human bone grafts for reconstructing head and face. Stem Cells Transl Med **1,** 64, 2012.
2. Warnke, P.H., Wiltfang, J., Springer, I., Acil, Y., Bolte, H., Kosmahl, M., *et al.* Man as living bioreactor: fate of an exogenously prepared customized tissue-engineered mandible. Biomaterials **27,** 3163, 2006.
3. Warnke, P.H., Springer, I.N., Wiltfang, J., Acil, Y., Eufinger, H., Wehmoller, M., *et al.* Growth and transplantation of a custom vascularised bone graft in a man. Lancet **364,** 766, 2004.
4. Terheyden, H., Knak, C., Jepsen, S., Palmie, S., and Rueger, D.R. Mandibular reconstruction with a prefabricated vascularized bone graft using recombinant human osteogenic protein-1: an experimental study in miniature pigs. Part I: prefabrication. Int J Oral Maxillofac Surg **30,** 373, 2001.
5. Alam, M.I., Asahina, I., Seto, I., Oda, M., and Enomoto, S. Prefabrication of vascularized bone flap induced by recombinant human bone morphogenetic protein 2 (rhBMP-2). Int J Oral Maxillofac Surg **32,** 508, 2003.
6. Becker, S.T., Bolte, H., Krapf, O., Seitz, H., Douglas, T., Sivananthan, S., *et al.* Endocultivation: 3D printed customized porous scaffolds for heterotopic bone induction. Oral Oncol **45,** e181, 2009.
7. Terheyden, H., Jepsen, S., and Rueger, D.R. Mandibular reconstruction in miniature pigs with prefabricated vascularized bone grafts using recombinant human osteogenic protein-1: a preliminary study. Int J Oral Maxillofac Surg **28,** 461, 1999.
8. Terheyden, H., Menzel, C., Wang, H., Springer, I.N., Rueger, D.R., and Acil, Y. Prefabrication of vascularized bone grafts using recombinant human osteogenic protein-1—part 3: dosage of rhOP-1, the use of external and internal scaffolds. Int J Oral Maxillofac Surg **33,** 164, 2004.
9. Warnke, P.H., Springer, I.N., Acil, Y., Julga, G., Wiltfang, J., Ludwig, K., *et al.* The mechanical integrity of in vivo engineered heterotopic bone. Biomaterials **27,** 1081, 2006.
10. Heliotis, M., Lavery, K.M., Ripamonti, U., Tsiridis, E., di Silvio L. Transformation of a prefabricated hydroxyapatite/osteogenic protein-1 implant into a vascularised pedicled bone flap in the human chest. Int J Oral Maxillofac Surg **35,** 265, 2006.
11. Hollister, S.J., and Murphy, W.L. Scaffold translation: barriers between concept and clinic. Tissue Eng Part B Rev **17,** 459, 2011.
12. Williams, J.M., Adewunmi, A., Schek, R.M., Flanagan, C.L., Krebsbach, P.H., Feinberg, S.E., *et al.* Bone tissue engineering using polycaprolactone scaffolds fabricated via selective laser sintering. Biomaterials **26,** 4817, 2005.
13. Wong, D.Y., Hollister, S.J., Krebsbach, P.H., and Nosrat, C. Poly(epsilon-caprolactone) and poly (L-lactic-co-glycolic acid) degradable polymer sponges attenuate astrocyte response and lesion growth in acute traumatic brain injury. Tissue Eng **13,** 2515, 2007.
14. Fitzsimmons, J. 510(k) Premarket Notification, Cover, Burr Hole, TRS Cranial Bone Void Filler. 2014. Available at: www.accessdata.fda.gov/scripts/cdrh/cfdocs/cfpmn/pmn.cfm?ID=K123633. Accessed March 8, 2014.
15. Yeo, A. 510(k) Premarket Notification, Methyl Methacrylate for Cranioplasty, Osteopore PCL Scaffold. 2014. Available at: www.accessdata.fda.gov/scripts/cdrh/cfdocs/cfpmn/pmn.cfm?ID=K051093. Accessed March 8, 2014.
16. Patel, J.J., Flanagan, C.L., and Hollister, S. Bone morphogenetic protein-2 adsorption onto poly-E-caprolactone better preserves bioactivity in vitro and produces more bone in vivo than conjugation under clinically relevant loading scenarios. Tissue Eng Part C Methods **21,** 489, 2015.
17. Holstein, J.H., Menger, M.D., Scheuer, C., Meier, C., Culemann, U., Wirbel, R.J., *et al.* Erythropoietin (EPO): EPO-receptor signaling improves early endochondral ossification and mechanical strength in fracture healing. Life Sci **80,** 893, 2007.
18. McGee, S.J., Havens, A.M., Shiozawa, Y., Jung, Y., and Taichman, R.S. Effects of erythropoietin on the bone microenvironment. Growth Factors **30,** 22, 2012.
19. Shiozawa, Y., Jung, Y., Ziegler, A.M., Pedersen, E.A., Wang, J., Wang, Z., *et al.* Erythropoietin couples hematopoiesis with bone formation. PLoS One **5,** e10853, 2010.
20. Kim, J., Jung, Y., Sun, H., Joseph, J., Mishra, A., Shiozawa, Y., *et al.* Erythropoietin mediated bone formation is regulated by mTOR signaling. J Cell Biochem **113,** 220, 2012.
21. Bakhshi, H., Rasouli, M.R., and Parvizi, J. Can local Erythropoietin administration enhance bone regeneration in osteonecrosis of femoral head? Med Hypotheses **79,** 154, 2012.
22. Haroon, Z.A., Amin, K., Jiang, X., and Arcasoy, M.O. A novel role for erythropoietin during fibrin-induced wound-healing response. Am J Pathol **163,** 993, 2003.
23. Ribatti, D. Erythropoietin and tumor angiogenesis. Stem Cells Dev **19,** 1, 2010.
24. Saray, A., Ozakpinar, R., Koc, C., Serel, S., Sen, Z., and Can, Z. Effect of chronic and short-term erythropoietin treatment on random flap survival in rats: an experimental study. Laryngoscope **113,** 85, 2003.
25. Maiese, K., Chong, Z.Z., and Shang, Y.C. Raves and risks for erythropoietin. Cytokine Growth Factor Rev **19,** 145, 2008.
26. Kobayashi, H., Minatoguchi, S., Yasuda, S., Bao, N., Kawamura, I., Iwasa, M., *et al.* Post-infarct treatment with an erythropoietin-gelatin hydrogel drug delivery system for cardiac repair. Cardiovasc Res **79,** 611, 2008.
27. Chen, F., Liu, Q., Zhang, Z.D., and Zhu, X.H. Co-delivery of G-CSF and EPO released from fibrin gel for therapeutic neovascularization in rat hindlimb ischemia model. Microcirculation **20,** 416, 2013.
28. Sun, H., Jung, Y., Shiozawa, Y., Taichman, R.S., and Krebsbach, P.H. Erythropoietin modulates the structure of bone morphogenetic protein 2-engineered cranial bone. Tissue Eng Part A **18,** 2095, 2012.
29. Nair, A.M., Tsai, Y.T., Shah, K.M., Shen, J., Weng, H., Zhou, J., *et al.* The effect of erythropoietin on autologous stem cell-mediated bone regeneration. Biomaterials **34,** 7364, 2013.
30. Haller, H., Christel, C., Dannenberg, L., Thiele, P., Lindschau, C., and Luft, F.C. Signal transduction of erythropoietin in endothelial cells. Kidney Int **50,** 481, 1996.
31. Anagnostou, A., Lee, E.S., Kessimian, N., Levinson, R., and Steiner, M. Erythropoietin has a mitogenic and positive chemotactic effect on endothelial cells. Proc Natl Acad Sci U S A **87,** 5978, 1990.
32. Desai, A., Zhao, Y., Lankford, H.A., and Warren, J.S. Nitric oxide suppresses EPO-induced monocyte chemoattractant protein-1 in endothelial cells: implications for atherogenesis in chronic renal disease. Lab Invest **86,** 369, 2006.

33. Cahill, K.S., Chi, J.H., Day, A., and Claus, E.B. Prevalence, complications, and hospital charges associated with use of bone-morphogenetic proteins in spinal fusion procedures. JAMA **302,** 58, 2009.
34. Santo, V.E., Gomes, M.E., Mano, J.F., and Reis, R.L. Controlled release strategies for bone, cartilage, and osteochondral engineering—part I: recapitulation of native tissue healing and variables for the design of delivery systems. Tissue Eng Part B Rev **19,** 308, 2013.
35. Luksenburg, H., Weir, A., and Wager, R. 2004. Safety concerns associated with Aranesp (darbepoetin alfa) Amgen, Inc. and Procrit (epoetin alfa) Ortho Biotech, L.P., for the treatment of anemia associated with cancer chemotherapy. Available at: www.fda.gov/ohrms/dockets/ac/04/briefing/4037b2_04_fda-aranesp-procrit.htm. Accessed October 9, 2014.
36. Amgen Initiates Voluntary Nationwide Recall of Certain Lots Of Epogen® And Procrit® (Epoetin Alfa). 2013. Available at: www.fda.gov/Safety/Recalls/ucm227202.htm. Accessed October 9, 2014.
37. Wang, T., Jiang, X.J., Lin, T., Ren, S., Li, X.Y., Zhang, X.Z., *et al.* The inhibition of postinfarct ventricle remodeling without polycythaemia following local sustained intramyocardial delivery of erythropoietin within a supramolecular hydrogel. Biomaterials **30,** 4161, 2009.
38. Kang, C.E., Poon, P.C., Tator, C.H., and Shoichet, M.S. A new paradigm for local and sustained release of therapeutic molecules to the injured spinal cord for neuroprotection and tissue repair. Tissue Eng Part A **15,** 595, 2009.
39. Fayed, B.E., Tawfik, A.F., and Yassin, A.E. Novel erythropoietin-loaded nanoparticles with prolonged in vivo response. J Microencapsul **29,** 650, 2012.
40. Bokharaei, M., Margaritis, A., Xenocostas, A., and Freeman, D.J. Erythropoietin encapsulation in chitosan nanoparticles and kinetics of drug release. Curr Drug Deliv **8,** 164, 2011.
41. Schroder, C.H., Swinkels, L.M., Reddingius, R.E., Sweep, F.G., Willems, H.L., and Monnens, L.A. Adsorption of erythropoietin and growth hormone to peritoneal dialysis bags and tubing. Perit Dial Int **21,** 90, 2001.

Address correspondence to:
Scott J. Hollister, PhD
Department of Biomedical Engineering
University of Michigan
1101 Beal Avenue
2214 Lurie Biomedical Engineering
Ann Arbor, MI 48109-2110

E-mail: scottho@umich.edu

Received: November 20, 2014
Accepted: March 5, 2015
Online Publication Date: July 17, 2015

This article has been cited by:

1. Ahmad Jabir Rahyussalim, Aldo Fransiskus Marsetio, Tri Kurniawati. 2017. Bioreactor as a New Resource of Autologous Bone Graft to Overcome Bone Defect In Vivo. *Clinical Reviews in Bone and Mineral Metabolism* **15**:4, 139-150. [Crossref]
2. Elbay Malikmammadov, Tugba Endogan Tanir, Aysel Kiziltay, Vasif Hasirci, Nesrin Hasirci. 2017. PCL and PCL-based materials in biomedical applications. *Journal of Biomaterials Science, Polymer Edition* **9**, 1-31. [Crossref]
3. Sahar Hiram-Bab, Drorit Neumann, Yankel Gabet. 2017. Erythropoietin in bone – Controversies and consensus. *Cytokine* **89**, 155-159. [Crossref]
4. Sahar Hiram-Bab, Drorit Neumann, Yankel Gabet. Context-Dependent Skeletal Effects of Erythropoietin 161-179. [Crossref]
5. Ru-Lin Huang, Eiji Kobayashi, Kai Liu, Qingfeng Li. 2016. Bone Graft Prefabrication Following the In Vivo Bioreactor Principle. *EBioMedicine* **12**, 43-54. [Crossref]
6. D.W. Weisgerber, K. Erning, C.L. Flanagan, S.J. Hollister, B.A.C. Harley. 2016. Evaluation of multi-scale mineralized collagen–polycaprolactone composites for bone tissue engineering. *Journal of the Mechanical Behavior of Biomedical Materials* **61**, 318-327. [Crossref]
7. Ru-Lin Huang, Kai Liu, Qingfeng Li. 2016. Bone regeneration following the in vivo bioreactor principle: is in vitro manipulation of exogenous elements still needed?. *Regenerative Medicine* **11**:5, 475-481. [Crossref]
8. Jie Hao, Kenneth C. K. Cheng, Laura G. Kruger, Lena Larsson, James V. Sugai, Joerg Lahann, William V. Giannobile. 2016. Multigrowth Factor Delivery via Immobilization of Gene Therapy Vectors. *Advanced Materials* **28**:16, 3145-3151. [Crossref]
9. Sophia P. Pilipchuk, Alberto Monje, Yizu Jiao, Jie Hao, Laura Kruger, Colleen L. Flanagan, Scott J. Hollister, William V. Giannobile. 2016. Integration of 3D Printed and Micropatterned Polycaprolactone Scaffolds for Guidance of Oriented Collagenous Tissue Formation In Vivo. *Advanced Healthcare Materials* **5**:6, 676-687. [Crossref]
10. Peng Pei, Xin Qi, Xiaoyu Du, Min Zhu, Shichang Zhao, Yufang Zhu. 2016. Three-dimensional printing of tricalcium silicate/mesoporous bioactive glass cement scaffolds for bone regeneration. *Journal of Materials Chemistry B* **4**:46, 7452-7463. [Crossref]